





# Optimized MPPT for Aero-generator System built on Autonomous Squirrel Cage Generators Using Feed-Forward Neural Network

Ouafia Fadi\*, Ahmed Abbou\*, Hassane Mahmoudi, Soufiane Gaizen\*

\* Department of Electrical Engineering, Mohammadia School of Engineers (EMI), Mohammed V University, Rabat, Morocco  
([fadiouafia@gmail.com](mailto:fadiouafia@gmail.com), [abbou@emi.ac.ma](mailto:abbou@emi.ac.ma), [mahmoudi@emi.ac.ma](mailto:mahmoudi@emi.ac.ma), [soufiane.gaizen@gmail.com](mailto:soufiane.gaizen@gmail.com))

‡ Corresponding Author; Ouafia Fadi, 10090 Tel: +212 6 60 87 00 22, [fadiouafia@gmail.com](mailto:fadiouafia@gmail.com)

*Received: 09.02.2023 Accepted: 17.05.2023*

**Abstract-** The research on Maximum Power Point Tracking (MPPT) techniques for wind turbine installation (WTI) is an ongoing effort to improve the output power of wind systems. AI-based controllers, particularly Neural network controllers, are becoming popular choices for capturing maximum power from wind generators. However, obtaining accurate data for training and fine-tuning the Artificial Neural Network (ANN) model remains a significant challenge in establishing effective MPPT methods. Our study proposes a novel approach using feed-forward function neural networks (FF-NN) for MPPT in WTI based on Autonomous Squirrel Cage Generators (ASCGs). Our study contributes to the advancement of MPPT techniques in the wind energy industry by presenting a comprehensive comparative analysis of various MPPT techniques, including VSS-P&O, VSS-INC, OTC, GA, and GWO. The FF-NN approach maximizes MPPT by regulating the duty cycle and accurately tracking the maximum power point (MPP) without requiring knowledge of wind turbine power characteristics. The results of our simulations in the MATLAB/Simulink environment show that the FF-NN method performs better under diverse loads and environmental disturbances, sustains the ASCG's voltage build-up under severe loads, and has high responsiveness to noisy wind speeds. Moreover, our study highlights the improved performance metrics of using FF-NN, such as its lower complexity, easy maintenance, and better MPP tracking accuracy compared to the other MPPT techniques. The proposed approach using FF-NN is a novel and comprehensive solution that adds to the existing body of knowledge in the field of wind energy by presenting a new perspective for MPPT techniques in ASCG-based WTI.

**Keywords** ASCG; MPPT; FF-NN; OTC; VSS-INC; VSS-P&O; GA; GWO.

## 1. Introduction

Currently, wind energy is one of the most sought-after renewable energy sources for the production of electrical energy, both for remote localisations and as a supplement for integrated power distribution. It can be a competitive alternative, contributing to the reduction of the rapidly increasing demand for electricity. The development and proliferation of the use of wind energy conversion chains have led industrialists and scientists to invest in improving the technical and economic indices of this conversion and the quality of the energy supplied [1].

Most of the isolated wind systems prefer the use of asynchronous squirrel cage generators due to their low cost, robustness, and standardization [2]. These generators are often associated with a capacitor bank, which provides the reactive

power necessary for their magnetization. When an ASCG is excited with a constant mechanical energy source, capacitor banks are a convenient solution for providing reactive power for its excitation to build up the voltage, as explained in [3].

In fact, the rotor's speed changes due to the change of mechanical energy source, which also modifies the values of several variables in the ASCG and requires a new calculation of the excitation according to the varied rotor speed. As explained in [4], the use of capacitors as an excitation source in the case of variable rotor speed is severely restricted. This is because the connected capacitance has a highly nonlinear dependence and does not alter dynamically in response to the variable rotor speed.

Producing electricity from a variable mechanical energy source, such as wind, requires systems for detecting and

tracking the generator's maximum power point (MPP) as they can work over a wide range of random speeds. Several works have [5] addressed the problem of optimizing wind power generation, using different MPPT techniques. These techniques differ according to the type of information they need to deliver the speed reference. The classification of these techniques into various families is determined by their operational characteristics, specifically, whether they require wind speed and aerodynamic features to generate the reference for maximizing power output or not.

As explained in [6], the Tip Speed Ratio - TSR is a kind of control that regulates wind turbine rotation speed to maintain the speed ratio at its optimum level ( $\lambda_{opt}$ ). This means that the turbine speed  $\Omega_{turbine}$  will be varied as a function of the wind speed variations  $V$ , allowing it to work continuously with maximum aerodynamic efficiency. The first drawback of this method is its strong dependence on the wind speed measurement; the quality of the wind image provided by the anemometer presents difficulties in practical implementations [7]. Abdullah, M. [8] claims that the TSR approach is straightforward, but measuring wind speed continually and precisely complicates the system and raises the cost. The second drawback is the need to obtain the optimal value of speed ratio  $\lambda_{opt}$ , which is different from one system to another. The consequence of this dependence on the wind generator characteristics is that each wind turbine must have its own adapted management software. To avoid the measurement of wind speed, the optimal torque control (OTC) controls the torque to its optimum in order to obtain the maximum value of the power coefficient and, therefore, maximum energy efficiency without the use of a wind speed sensor. However, this control requires knowledge of the maximum power curve of the wind turbine [9,10].

Each of the OTC and TSR methods is directly or indirectly reliant on the characteristics of the wind generator, which leads to difficulties in the implementation of these methods and additional costs for the system. To overcome these issues, there are several methods to determine the operating points without knowing the aerodynamic characteristics curve. For instance, Perturb & Observe (P&O), the principle of this technique consists in adjusting the operating point by perturbing the system's operating voltage or current and comparing the resulting change in power to determine the direction of the next perturbation. The method has a relatively simple implementation, but it may lead to oscillations around the MPP and can be slow to converge when the operating point is far from the MPP. To address this issue, the variable step size (VSS-P&O) adjusts the step size of the perturbation based on the rate of change of power output, which leads to faster and more accurate convergence towards the MPP. However, this method can be more complex to implement because it requires additional algorithms to determine the step size, and it needs to be adjusted dynamically based on the tracking performance [11].

On the other hand, the INC method adjusts the operating point by calculating incremental conductance, which is the ratio of the change in power to the change in voltage or current [12]. The operating point is adjusted in the direction that maximizes the incremental conductance using a fixed step

size, whereas the variable step size (VSS-INC) calculates the incremental conductance at each step and adjusts the step size in proportion to the change in conductance. This results in faster convergence towards the MPP and reduced oscillation around the MPP. However, both methods are more complex and require additional circuitry to prevent false triggering due to noise and measurement errors [13].

Recently, fuzzy logic control has been used in maximum power point tracking (MPPT) systems [14]. Unlike conventional MPPT methods, the step change of the reference speed  $\Delta\Omega_{ref}$  is not constant. This sampling step was chosen in order to find a compromise between a fast search for the optimum and low oscillations around this optimum in a steady state. In addition, this control offers other advantages: it does not require exact knowledge of the model to be controlled, does not depend on the parameters of the system nor on the climatic parameters, and can deal with non-linearities. Despite this, there is still a problem with choosing the right membership functions, and a lot of calculations and data storage are needed. Additionally, simulations or experimental testing are necessary to figure out the maximum power curve, making implementation expensive and difficult [15].

According to advanced studies and surveys [16,17], smart maximum power point tracking algorithms can exploit the benefits of traditional approaches while eliminating their shortcomings. Therefore, a strong control approach is proposed in this study to enhance the efficiency of MPPT in WTIs, which employs an adaptive strategy using an FF-NN. The proposed method optimizes the duty cycle to attain the MPP. The FF-NN is a simpler structure providing a more robust and adaptable control system. In addition, the boost converter duty cycle is regulated by the FF-NN utilizing voltage and current as inputs, making the need for knowledge of the wind turbine's characteristics unnecessary. Thus, this MPPT control technique eliminates the requirement for anemometer or tachometer sensors to measure wind speed or turbine speed, resulting in a more cost-effective approach. This control strategy results in efficient MPPT and has the best tracking. Comparative studies with VSS-P&O, VSS-INC, OTC, GA, and GWO techniques are conducted to evaluate the performance of the proposed approach.

The paper is structured as follows: section 2 outlines the configuration of the whole wind power system; Section 3 provides a comprehensive overview of both typical and advanced Maximum Power Point Tracking (MPPT) techniques; Section 4 presents the simulation findings in detail, while section 5 offers conclusive remarks.

## 2. WTI modeling section

The system depicted in Fig. 1 displays the configuration of a WTI that utilizes an ASCG. This configuration consists of a wind turbine that is linked to an autonomous squirrel cage generator. To transform the AC voltage from the wind turbine to DC voltage, a three-phase diode rectifier is employed. Additionally, the DC/DC converter is regulated by a Pulse Width Modulation (PWM) signal from the MPPT controller, which assesses the wind generator's output voltage and current to determine the suitable PWM signal

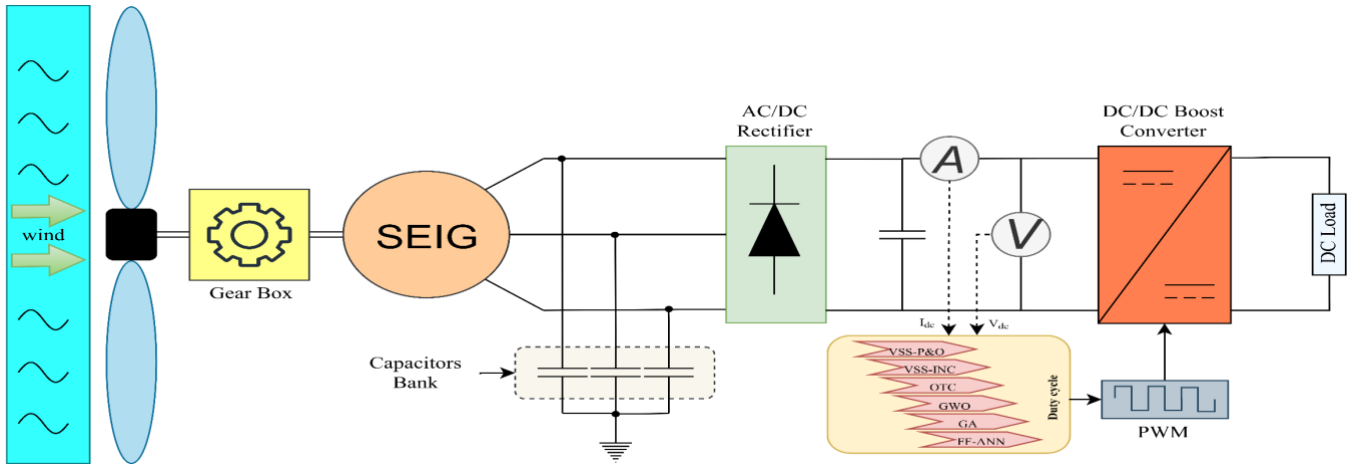


**Fig. 1.** Set-up of the aero-generator conversion plant

**2.1 Autonomous squirrel cage generator setup modeling**

The determination of adequate capacitance to ensure the priming of the machine has been studied in several kinds of research [3,4]. The modeling of the ASCG’s magnetization is translated by taking into account the variation of the magnetizing inductance  $L_m$ , which is necessary to satisfy the accumulation and stabilization of the stator output voltage [4].

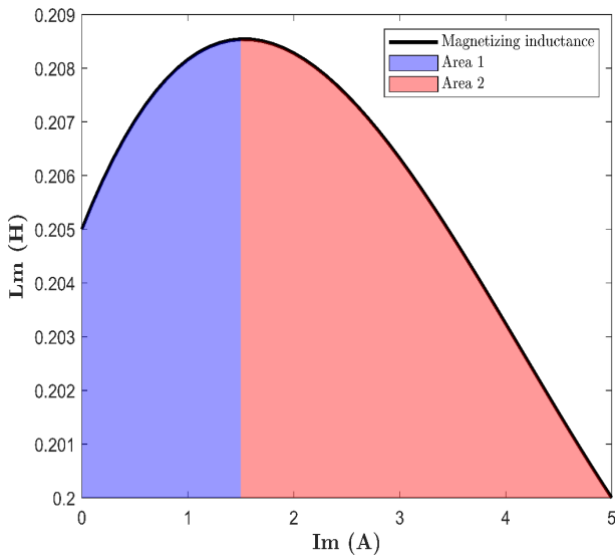


**Fig.2.** Variation of magnetizing inductance  $L_m$  with excitation current in ASCG

According to Fig. 2, it is obvious that  $L_m$  is initially close to 0.205H when the excitation current is near zero. As self-excitation begins, the generated current increases, leading to an increase in  $L_m$ . This, in turn, causes the generated current to grow faster. The magnetizing inductance then starts to decrease while the current continues to grow until it reaches its steady-state value, which is determined by the  $L_m$  value, excitation capacitance, and rotor speed. The global matrix form of the squirrel-cage asynchronous machine in a d-q reference frame, taking into account magnetic saturation, is written as follows [18]:

$$\begin{pmatrix} R_s + sL_s + \frac{1}{sC} & 0 & sL_m & 0 \\ 0 & R_s + sL_s + \frac{1}{sC} & 0 & sL_m \\ sL_m & -\omega_r L_m & R_r + sL_r & -\omega_r L_r \\ \omega_r L_m & sL_m & \omega_r L_r & R_r + sL_r \end{pmatrix} \begin{pmatrix} i_{qs} \\ i_{ds} \\ i_{qr} \\ i_{dr} \end{pmatrix} + \begin{pmatrix} V_{cq0} \\ V_{cd0} \\ -K_{qr} \\ K_{dr} \end{pmatrix} = \begin{pmatrix} 0 \\ 0 \\ 0 \\ 0 \end{pmatrix} \quad (1)$$

Where  $R_s$  and  $R_r$  denote the per-phase resistances of the stator and rotor, correspondingly.

$L_s$  and  $L_r$  represent the per-phase inductances of the stator and rotor, successively.

$i_{ds}$  and  $i_{qs}$  represent the stator current in the d-axis and q-axis, respectively.

$i_{dr}$  and  $i_{qr}$  represent the rotor current on the d-axis and q-axis, respectively.

$K_{dr}$  and  $K_{qr}$  represent induced voltages resulting from residual magnetizing flux along the d-axis and q-axis, respectively.

$V_{cd0}$  and  $V_{cq0}$  represent the initial voltages along the d-axis and q-axis, respectively.

The electromagnetic torque is given by:

$$T_e = 1.5p(\varphi_{ds}i_{qs} - \varphi_{qs}i_{ds}) \quad (2)$$

$$\varphi_{qs} = L_s i_{qs} + L_m i_{qr} \quad (3)$$

$$\varphi_{ds} = L_s i_{ds} + L_m i_{dr} \quad (4)$$

Where  $T_e$  represents the electromagnetic torque produced by the ASCG.

$\varphi_{ds}$ ,  $\varphi_{qs}$  represent stator flux along the d-axis and q-axis, respectively.

$p$  represents the pole pairs number.

The mechanical torque of the aero-generator driven induction generator is:

$$T_m = j \frac{dw}{dt} + Dw + T_e \quad (5)$$

Where J denotes the inertial coefficient.

D is the combined friction coefficient of the gearbox and generator.

T<sub>m</sub> represents the mechanical torque of the aero generator.

### 2.2 Wind turbine modeling

The power produced by the aerogenerator can be written as follows [19]:

$$P_v = \frac{1}{2} * A * \rho * V_{wind}^3 \quad (6)$$

Where P<sub>v</sub> represents the power produced by a wind turbine.

A represents the area covered by the blades [m<sup>2</sup>].

ρ represents the air density, approximately 1.3 kg/m<sup>3</sup>.

V<sub>wind</sub> represents the wind speed [m/s].

The turbine modeling entails simulating the turbine's mechanical power and torque, which are supplied by [19]:

$$P_m = C_p * P_v = C_p(\lambda, \beta) * \frac{1}{2} * A * \rho * V_{wind}^3$$

$$= \frac{1}{2} * \rho * \pi * R^2 * V_{wind}^3 * C_p(\lambda, \beta) \quad (7)$$

$$T_m = \frac{P_m}{\Omega} = \frac{1}{2} * \rho * \pi * R^3 * V_{wind}^3 * T_t \quad (8)$$

where P<sub>m</sub> is the mechanical power.

C<sub>p</sub> represents the power coefficient.

λ represents the tip speed ratio.

β represents the pitch angle.

R represents the radius of a wind turbine blade [m].

Generally, there are several articles that present the coefficient C<sub>p</sub> by graphs [19]. The C<sub>p</sub> coefficient is different from one turbine to another, and is usually provided by the designer and can be used to define a mathematical approximation. The power coefficient C<sub>p</sub> represents the aerodynamic efficiency, its value relies on the tip speed ratio λ and the Pitch angle β.

$$C_p(\lambda, \beta) = c_1(c_2/\lambda_i - c_3\beta - c_4)e^{-c_5/\lambda_i} + c_6\lambda \quad (9)$$

With:

$$\frac{1}{\lambda_i} = \frac{1}{\lambda + 0.08\beta} - \frac{0.035}{\beta^3 + 1} \quad (10)$$

The coefficients c<sub>1</sub> through c<sub>6</sub> are: c<sub>1</sub>= 0.5176, c<sub>2</sub>=116, c<sub>3</sub>=0.4, c<sub>4</sub>=5, c<sub>5</sub>= 21 and c<sub>6</sub>=0.0068.

As illustrated in Fig.3, the peak value of C<sub>p</sub> (C<sub>pmax</sub>=0.48) is achieved for β=0 and for λ = 8.1. This particular value of λ is defined as the nominal value λ<sub>nom</sub>.

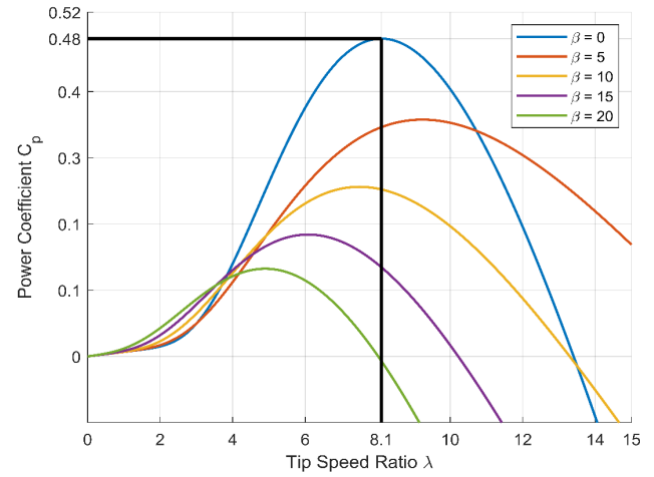


**Fig.3.:** Characteristic of C<sub>p</sub> as a function of λ for different values of the Pitch angle β

The tip speed ratio λ is wind turbine's particular factor, defined as [19].

$$\lambda = \frac{\Omega * R}{V_{wind}} \quad (11)$$

Where Ω represents the angular velocity of the rotor [rad/s].

### 2.3 DC/DC Boost converter modeling

As illustrated in Fig.4, the basic circuit of a boost converter consists of an inductor L, a semiconductor switch (MOSFET), a diode, and a capacitor [20].

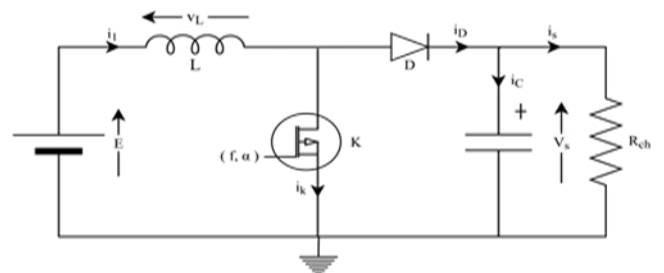


**Fig.4.** Circuit equivalent of a boost converter

The parameters that define this converter are sized as follows:

#### ➤ Duty cycle:

The operating duty cycle α is defined by the fraction [21]:

$$\alpha = 1 - \frac{E * \eta}{V_s} \quad (12)$$

Where V<sub>s</sub> and E represent the output and the input voltages of the DC/DC converter, respectively.

η stands for the converter's effectiveness.

➤ **Inductor calculation:**

The calculation of the inductance begins with the calculation of the maximum input current [21]:

$$\Delta I_L = \frac{\alpha * E * T}{L} = \frac{\alpha * E}{L * f} \quad (13)$$

$$L = \frac{\alpha * E}{f * \Delta I_L} \quad (14)$$

Where  $\Delta I_L$  represents inductor ripples, and  $f$  represents the switching frequency.

➤ **Capacitor calculation:**

During phase 1, which lasts  $\alpha T$ , the capacitor provides the energy to the load. We can write [21]:

$$C * \frac{dV_s}{dt} = -I_s \quad (15)$$

Assuming the output current is constant, we can calculate the charge supplied by the capacitor, which is equal to:

$$\Delta Q = I_s * \alpha * T \quad (16)$$

We admit a ripple in the output voltage,  $\Delta V_s$ , to be written as:

$$\Delta Q = C * \Delta V_s \quad (17)$$

To deduce the capacitance:

$$C = \frac{I_s * \alpha * T}{\Delta V_s} = \frac{\alpha * I_s}{f * \Delta V_s} \quad (18)$$

**3. Advanced MPPT algorithms section**

**3.1 Variable Step Size Perturb and Observe (VSS-P&O)-based MPPT algorithm.**

The variable step size perturbs and observe (VSS-P&O) algorithm works by continuously perturbing the operating point of the wind turbine and observing the resulting power output, as shown in Fig.5. The perturbations are carried out by changing the duty cycle of the power converter, which affects the voltage and current of the system. The algorithm then calculates the instantaneous power output of the wind turbine, based on the measured voltage and current, and compares it with the previous power output. If the new power output is higher, the algorithm continues perturbing in the same direction, but with a smaller step size. If the new power output is lower, the algorithm perturbs in the opposite direction with a larger step size. This way, the step size of the algorithm is adjusted dynamically based on the response of the system, improving tracking accuracy and reducing oscillations around the maximum power point (MPP). Compared to fixed step P&O algorithms, which use a fixed step size for perturbation, the variable-step P&O algorithm can adapt to changing wind speed conditions more efficiently, resulting in improved energy conversion efficiency [11].

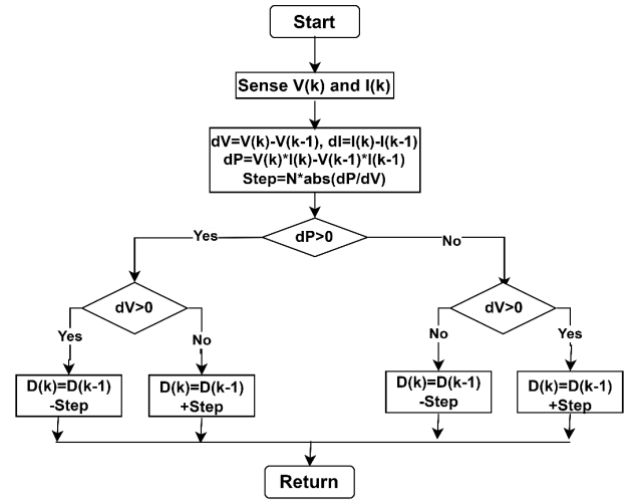


Fig.5.: Outline of VSS-P&O algorithm

**3.2 Variable Step Size Incremental Conductance (VSS-INC)-based MPPT algorithm**

The variable step size incremental conductance (VSS-INC) algorithm is another popular maximum power point tracking (MPPT) technique used in wind energy conversion systems. Similar to the variable step perturb and observe (P&O) algorithm, the variable step INC algorithm adjusts the step size dynamically based on the system's response. However, instead of comparing the instantaneous power output with the previous power output as in the P&O algorithm, the variable step INC algorithm compares the incremental conductance, which is the change in power with respect to the change in voltage. When the incremental conductance is zero, the system is operating at the MPP, as shown in Fig.6. The variable step INC algorithm then adjusts the duty cycle of the power converter accordingly to maintain the system at the MPP. Compared to fixed-step INC algorithms, which use a fixed step size for adjusting the duty cycle, the variable-step INC algorithm can track the MPP more accurately and efficiently under changing wind speed conditions, leading to improved energy conversion efficiency [13].

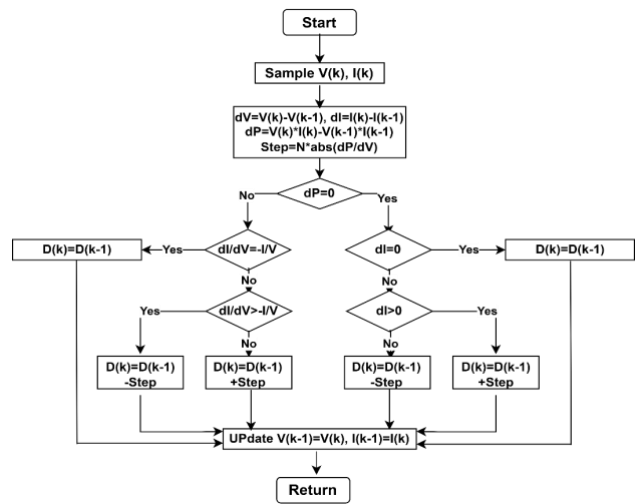


Fig.6.: Outline of VSS-INC algorithm

3.3 Optimal torque control (OTC) based-MPPT algorithm.

The optimal torque control (OTC) algorithm is a maximum power point tracking (MPPT) technique that aims to extract maximum power from the wind turbine by controlling the generator's torque. The algorithm uses the wind turbine's aerodynamic characteristics and the generator's electromagnetic properties to determine the optimal torque for maximum power extraction, as shown in Fig.7. The algorithm calculates the optimal torque based on the wind speed, the blade pitch angle, and the generator's electrical parameters. Once the optimal torque is determined, the algorithm adjusts the generator's torque by controlling the generator's rotor speed or the blade pitch angle to maintain the system at the MPP. The OTC algorithm has been shown to be effective in improving energy conversion efficiency, particularly in variable wind speed conditions. However, the algorithm's implementation requires accurate knowledge of the wind turbine's aerodynamic and electromagnetic properties, which can be challenging to obtain [9,10].

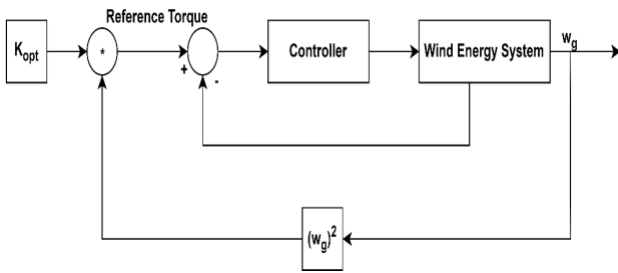


Fig.7.: Outline of OTC description

3.4 Feed forward Neural network (FF-NN) based MPPT algorithm.

In this study, a Feedforward Neural Network (FF-NN) controller was utilized to train the Maximum Power Point Tracking (MPPT) controller. This approach offers significant advantages over traditional methods by effectively handling non-linearities, time-varying behavior, and uncertainties in both wind turbines and wind speed. Consequently, the tracking of maximum power points is quicker, and power extraction efficiency is higher [22].

The FF-NN model is designed with a simple architecture comprising an input layer, two hidden layers with multiple neurons, and an output layer, as shown in Fig.8. It uses voltage and current as input variables and the duty cycle of the boost converter as an output variable. A large dataset is used to train the FF-NN model, which determines the optimal duty cycle for maximum power output [23,24].

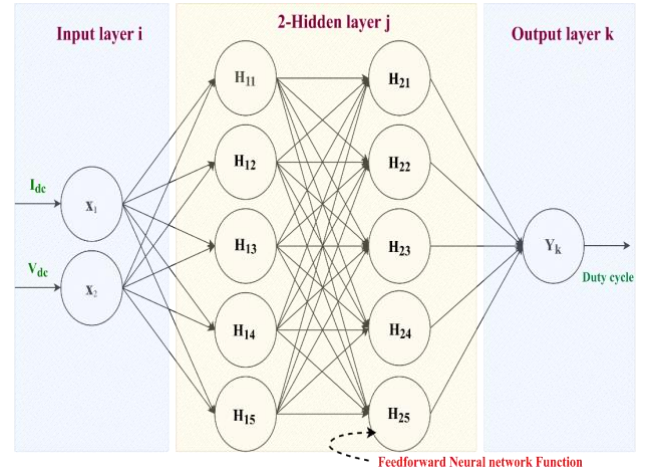


Fig.8.: Outline of Feedforward Neural network algorithm

3.5 Grey wolf optimizer based MPPT Algorithm

In this study, the Grey Wolf Optimizer (GWO) algorithm was employed to design a Maximum Power Point Tracking (MPPT) control for an aerogenerator linked to a boost converter. The objective function was defined as the negative value of the wind turbine's output power at duty cycle D, which was considered the input parameter for the algorithm.

The algorithm, as illustrated in Fig.9, was initialized with a population of N grey wolves, each with a randomly generated position vector in the duty cycle search space. The fitness of each wolf was evaluated using the sigmoid function, and the position of each wolf was updated using the equations below. The duty cycle was then calculated for each new position using a sigmoid function, and the fitness was re-evaluated. The alpha, beta, and delta wolves were identified based on their fitness, and the process was repeated until convergence.

Finally, the duty cycle of the alpha wolf was determined as the optimal duty cycle to ensure that the wind turbine operates at its highest level of efficiency [25,26].

$$D_{\alpha} = X_{\alpha} - A * (X_{\beta} - X_{\delta}) \tag{19}$$

$$D_{\beta} = X_{\beta} - A * (X_{\alpha} - X_{\delta}) \tag{20}$$

$$D_{\delta} = X_{\delta} - A * (X_{\alpha} - X_{\beta}) \tag{21}$$

$X_{\alpha}$ ,  $X_{\beta}$ , and  $X_{\delta}$  represent the position vectors of the  $\alpha$ ,  $\beta$ , and  $\delta$  wolves, respectively.

A is a coefficient used in the update equation to control the movement of the wolves during the search process.

$D_{\alpha}$ ,  $D_{\beta}$ , and  $D_{\delta}$  represent the duty cycle of the  $\alpha$ ,  $\beta$ , and  $\delta$  wolves, respectively, which are calculated based on their updated positions using the sigmoid function.

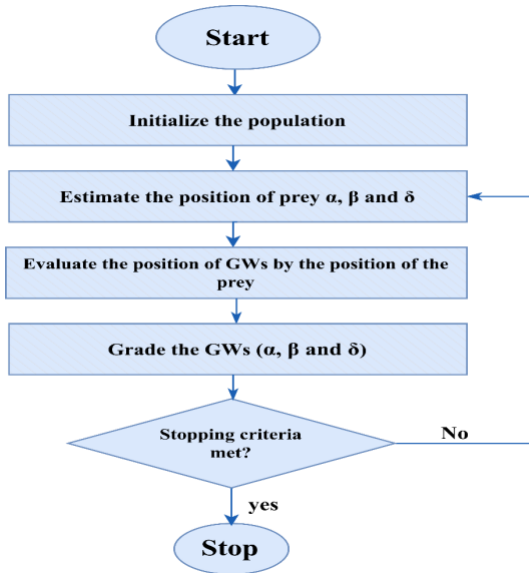


Fig.9.: Outline of Grey Wolf Optimizer Algorithm

3.6 Genetic algorithm-based MPPT

In this study, a Genetic Algorithm (GA) was employed to design a Maximum Power Point Tracking (MPPT) control for an aero-generator connected to a boost converter, where the input variables were the values of  $I_{dc}$  and  $V_{dc}$ . The objective function aimed to maximize the power output of the wind turbine at the duty cycle  $D$ , which was the output variable.

The GA algorithm, shown in Fig.10, initiated with a population of  $N$  individuals, and the fitness of each individual was evaluated based on the objective function. The selection, crossover, and mutation operators were applied to generate new individuals until the convergence criteria were met. Finally, the individual with the highest fitness value was determined as the optimal duty cycle to maintain the wind turbine at its maximum power point [27,28].

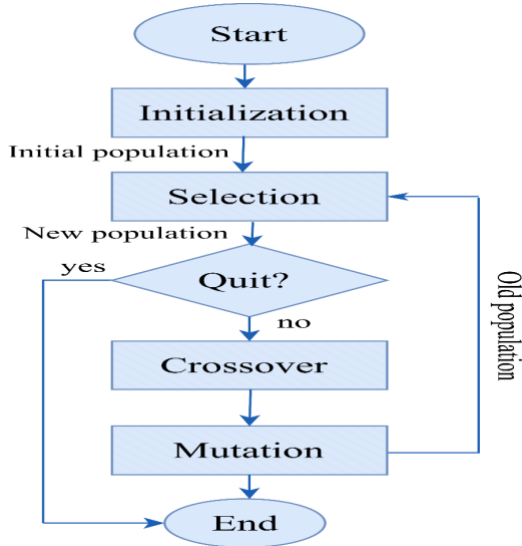


Fig.10. Outline of Genetic Algorithm

4. Simulation results section

This study investigates various MPPT techniques, including VSS-P&O, VSS-INC, OTC, GWO, GA, and FF-NN. The simulation tests involve comparing the performance of these algorithms under fixed and variable conditions (wind speed/load) and examining the effect of MPPT techniques on the voltage buildup of the ASCG.

4.1 Case 1: Wind speed constant

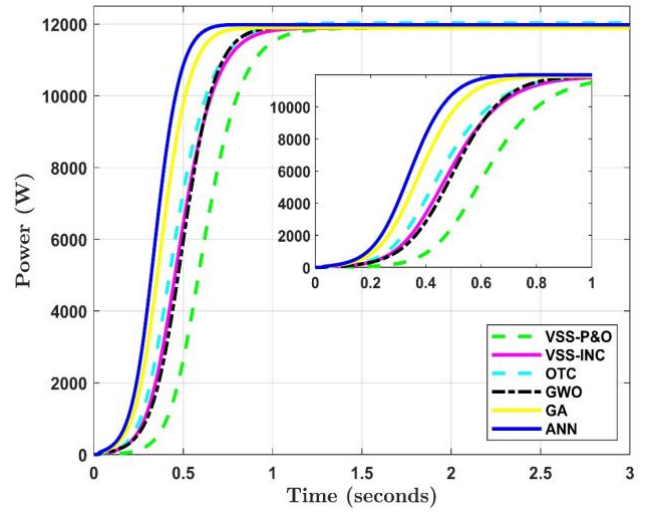


Fig.11. The DC power of the DC/DC boost converter performance for several MPPT approaches

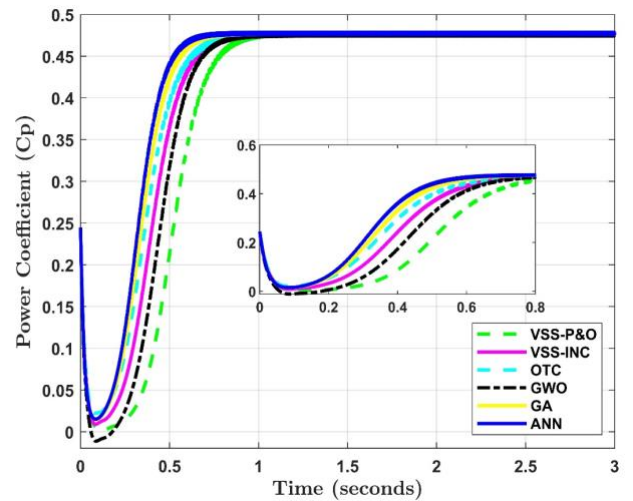


Fig.12. The Power Coefficient performance for several MPPT approaches

Figure 11 illustrates that all MPPT techniques were able to extract the maximum power from the wind turbine under a permanent wind speed condition. However, the MPPT technique based on FF-NN was found to reach the maximum power point (MPP) faster than other techniques, resulting in an increased overall energy yield of the system. This is due to FF-NN being a machine learning technique capable of learning patterns and relationships from data,

allowing it to predict the optimal operating point based on the current operating parameters. Conversely, other MPPT techniques such as GA and GWO utilize optimization algorithms that search for the optimal operating point using iterative calculations, which may take longer to converge to the MPP.

Additionally, the VSS-P&O technique was observed to have a slower response time compared to FF-NN as it changes the operating point in small steps and observes the change in power output. This process can take longer to converge to the MPP compared to FF-NN, which uses a more direct approach to predict the optimal operating point.

The Power Coefficient performance shown in Fig. 12 also supports this observation, where the use of feed-forward NN in the MPPT technique resulted in quicker attainment of power coefficient compared to other techniques.

4.2 Case 2: Variation of wind speed

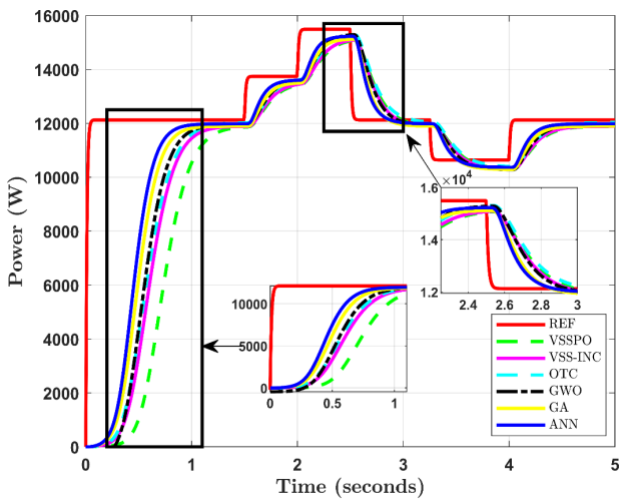


Fig.13. The DC power in the DC/DC boost converter under variable wind speed condition for several MPPT approaches

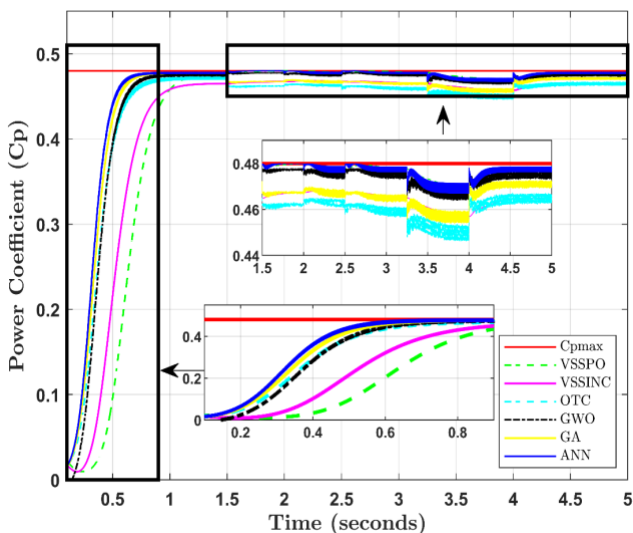


Fig.14. The power coefficient performance under variable wind speed condition for several MPPT approaches

The results presented in Fig.13 demonstrate that the feedforward neural network-based MPPT technique outperforms other techniques in terms of tracking and maintaining the maximum power point (MPP) of a wind turbine under variable wind speed conditions. Additionally, as depicted in Fig. 14, the FF-NN technique exhibits a faster response time and higher power coefficient than other techniques, indicating its ability to quickly adapt to changing operating conditions. While other MPPT techniques rely on iterative calculations or optimization algorithms, which can take longer to converge to the MPP and struggle to adapt to wind speed changes, the FF-NN technique's continuous tracking and maintenance of the MPP provide an advantage in maximizing power output.

4.3 Case 3: Variation of load

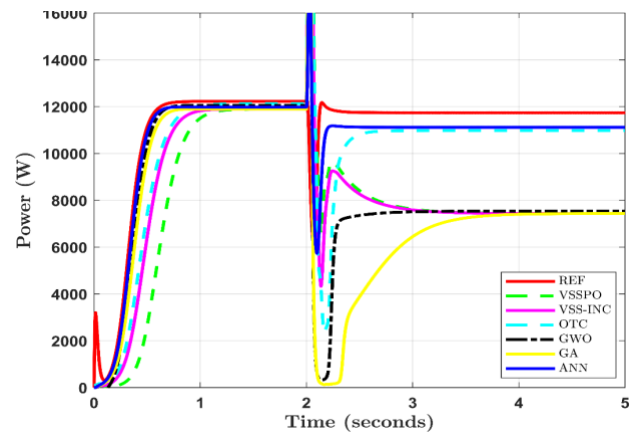


Fig.15. The DC power in the DC/DC boost converter under variable load condition for several MPPT approaches

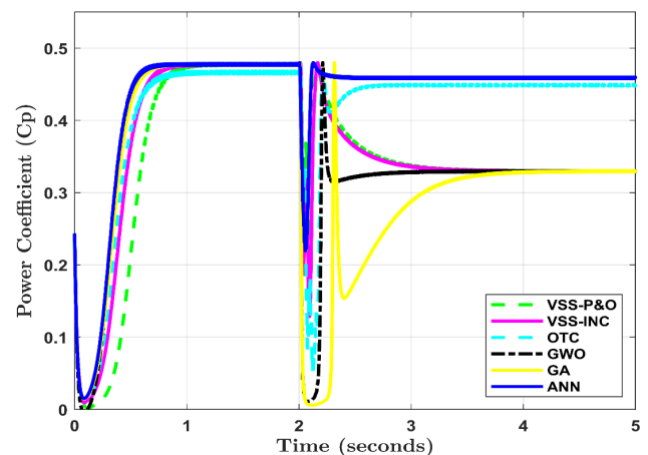
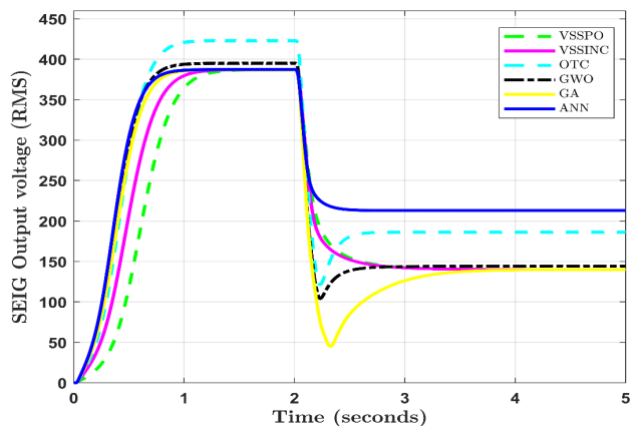


Fig.16. The power coefficient performance under variable load condition for several MPPT approaches

According to Fig. 15, all maximum power point tracking (MPPT) techniques were able to extract maximum power from a DC/DC boost converter prior to the application of load, with the FF-NN-based technique responding the fastest. However, after the load was applied, only the FF-NN and OTC-based techniques were able to maintain a stable output power by adjusting their operating



point, while the other techniques struggled due to their slower response time caused by heuristic search algorithms. These findings indicate that the choice of MPPT technique is crucial for stable output power under sudden load changes, with the FF-NN and OTC-based techniques being more suitable. Moreover, as shown in Fig.16, the FF-NN-based MPPT technique was able to maintain a higher power coefficient even after the load was applied. However, the OTC-based technique struggled to return the power coefficient to its maximum value and exhibited significant oscillations. The other MPPT techniques were also unable to maintain the power coefficient at its maximum value.



**Fig.17.** The RMS stator voltage build-up under extra-load condition for several MPPT approaches

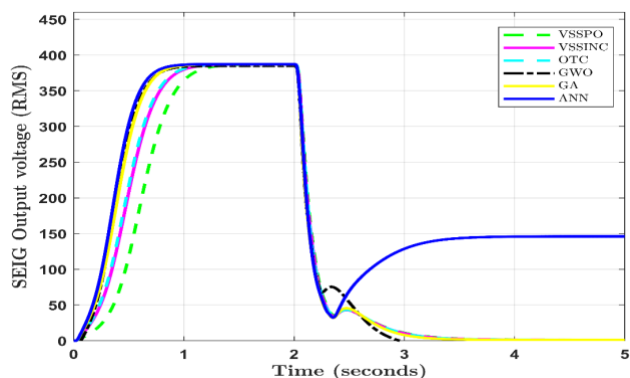


**Fig.18.** The RMS stator voltage build-up under extra-load condition for several MPPT approaches

In Fig. 17, it can be observed that all the maximum power point tracking (MPPT) techniques had a similar voltage build-up profile before applying the extra-load, except for the OTC-based technique, which had a slightly higher voltage build-up. However, after applying the extra-large load, the voltage build-up decreased for all the techniques. Interestingly, the FF-NN-based technique showed the highest voltage build-up, while the OTC-based technique had a slightly lower voltage build-up than the FF-NN-based technique, but still higher than the other techniques. However, in Fig.18, when applying an extra-large load, all the MPPT techniques experienced a loss in voltage build-up after the load change, except for the FF-NN-based technique, which was able to maintain a certain level of voltage build-up.

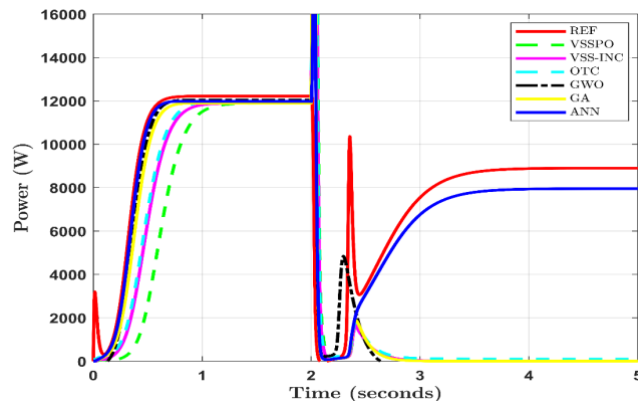


**Fig.19.** The DC power in the DC/DC boost converter under extra-large load condition for several MPPT approaches

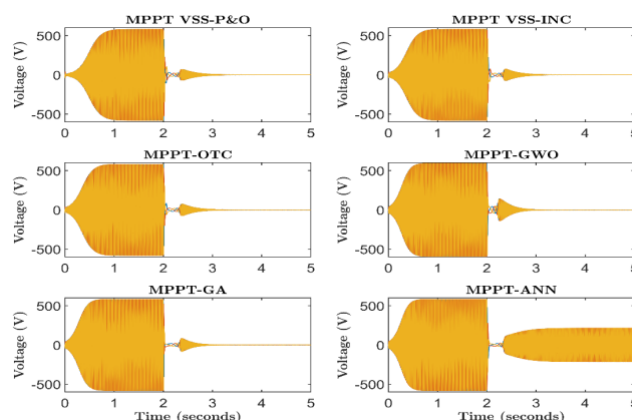


**Fig.20.** Three phase stator voltage build up under extra-large load for several MPPT approaches.

The output power of the DC-DC boost converter is presented in Fig. 19. Prior to applying the extra-large load, all MPPT techniques attained the maximum power point. However, after the load was added, all techniques lost MPP tracking and their voltage build-up, as shown in Fig. 20. The FF-NN-based technique was the only one that maintained a certain level of voltage build-up, allowing it to re-establish the MPP after making adjustments. This outcome emphasizes the significance of choosing appropriate MPPT techniques that can handle abrupt load changes and maintain a steady output power.

### 5. Conclusion

In conclusion, this study analyzes several MPPT techniques for wind energy conversion plants based on autonomous squirrel cage generators. The results show that the FF-NN-based controller is the most effective technique for extracting the highest power point of the aero-generator, while the FF-NN-based controller exhibits superior performance due to its ability to handle complex and non-linear systems, adapt to changes in wind speed, and efficiently handle different types of load and environmental disturbances. The simulation tests were conducted under fixed and variable conditions, and the FF-NN-based

approach consistently outperformed other techniques. Moreover, the FF-NN-based controller maintained the voltage buildup of the self-excited induction generator under heavy load, distinguishing it from other techniques. This study highlights the potential of artificial intelligence techniques in renewable energy systems and contributes to the advancement of wind energy technology for sustainable energy generation. The findings provide valuable insights for researchers and engineers seeking to optimize wind energy systems, particularly those based on self-excited induction generators, and emphasize the superior efficiency, adaptability, and reliability of the FF-NN-based approach.

## References

- [1] P. Sadorsky, "Wind energy for sustainable development: Driving factors and future outlook," *Journal of Cleaner Production*, vol. 289, p. 125779, 2021.
- [2] V.M. Krishna, V. Sandeep, S.S. Murthy, and K. Yadlapati, "Experimental investigation on performance comparison of self-excited induction generator and permanent magnet synchronous generator for small scale renewable energy applications," *Renewable Energy*, vol. 195, pp. 431-441, 2022.
- [3] W.A. Khan, M.N. Marsono, and M.A. Hannan, "Capacitance determination methods for self-excited induction generators: A review," *Renewable and Sustainable Energy Reviews*, vol. 137, 110622, 2021. Doi: 10.1016/j.rser.2020.110622.
- [4] F. Ouafia and A. Ahmed, "Elaboration of the Minimum Capacitor for an Isolated Self-Excited Induction Generator Driven by a Wind Turbine," in *International Conference of Computer Science and Renewable Energies*, pp. 264-270, 2018.
- [5] C.V. Govinda, S.V. Udhay, C. Rani, Y. Wang, and K. Busawon, "A Review on Various MPPT Techniques for Wind Energy Conversion System," in *International Conference on Computation of Power, Energy, Information and Communication (ICCPEIC)*, Chennai, India, pp. 310-326, 2018. Doi: 10.1109/ICCPEIC.2018.8525219.
- [6] Z. Dekali, L. Baghli, and A. Boumediene, "Speed controller efficiency of the TSR based MPPT of a variable speed wind power system," in *2022 2nd International Conference on Advanced Electrical Engineering (ICAEE)*, IEEE, 2022, pp. 1-5.
- [7] J. Pande, P. Nasikkar, K. Kotecha, and V. Varadarajan, "A review of maximum power point tracking algorithms for wind energy conversion systems," *Journal of Marine Science and Engineering*, vol. 9, no. 11, p. 1187, 2021.
- [8] S. Gautam, D.B. Raut, P. Neupane, D.P. Ghale, and R. Dhakal, "Maximum power point tracker with solar prioritize in photovoltaic application," in *2016 IEEE International Conference on Renewable Energy Research and Applications (ICRERA)*, IEEE, pp. 1051-1054, 2016.
- [9] S. Morimoto, H. Nakayama, M. Sanada, and Y. Takeda, "Sensorless output maximization control for variable-speed wind generation system using IPMSG," *IEEE Transactions on Industry Applications*, vol. 41, no. 1, pp. 60-67, 2005.
- [10] C. Maurizio and P. Marcello, "Growing neural gas (GNG)-based maximum power point tracking for high-performance wind generator with an induction machine," *IEEE Transactions on Industry Applications*, vol. 47, no. 2, pp. 861-872, 2011.
- [11] S.A. Mohamed and M. Abd El Sattar, "A comparative study of P&O and INC maximum power point tracking techniques for grid-connected PV systems," *SN Applied Sciences*, vol. 1, no. 2, p. 174, 2019.
- [12] A.I. Nusaif and A.L. Mahmood, "MPPT Algorithms (PSO, FA, and MFA) for PV System Under Partial Shading Condition, Case Study: BTS in Algazalia, Baghdad," *International Journal of Smart Grid-ijSmartGrid*, vol. 4, no. 3, pp. 100-110, 2020.
- [13] D. Haji and N. Genc, "Fuzzy and P&O based MPPT controllers under different conditions," in *2018 7th International Conference on Renewable Energy Research and Applications (ICRERA)*, IEEE, pp. 649-655, October 2018.
- [14] T. George, P. Jayapraksh, T. Francis, and C.E. Singh Sreedharan, "Wind energy conversion system based PMSG for maximum power tracking and grid synchronization using adaptive fuzzy logic control," *Journal of Applied Research and Technology*, vol. 20, no. 6, pp. 703-717, 2022.
- [15] O. Guenounou, A. Belkaid, I. Colak, B. Dahhou, and F. Chabour, "Optimization of fuzzy logic controller based maximum power point tracking using hierarchical genetic algorithms," in *2021 9th International Conference on Smart Grid (icSmartGrid)*, IEEE, pp. 207-211, June 2021.
- [16] T. Mitiku and M.S. Manshahia, "A Literature Review on the MPPT Techniques Applied in Wind Energy Harvesting System," in *Intelligent Computing & Optimization: Proceedings of the 4th International Conference on Intelligent Computing and Optimization 2021 (ICO2021)*, vol. 3, Springer International Publishing, 2022.
- [17] N. Sivakumar, A. Routray, N. Sajeev, F. Raju, and G. Dhiman, "Neural Network Based Reinforcement Learning for Maximum Power Extraction of Wind Energy," in *2022 IEEE 4th International Conference on Cybernetics, Cognition and Machine Learning Applications (ICCCMLA)*, IEEE, pp. 210-215, October 2022.

- [18] F. Ouafia and A. Ahmed, "A direct power control of the PWM rectifier for SEIG feeding resistive load in wind energy systems," in 2020 5th International Conference on Renewable Energies for Developing Countries (REDEC), IEEE, 2020.
- [19] K. Palanimuthu, G. Mayilsamy, S.R. Lee, S.Y. Jung, and Y.H. Joo, "Comparative analysis of maximum power extraction and control methods between PMSG and PMVG-based wind turbine systems," *International Journal of Electrical Power & Energy Systems*, vol. 143, p. 108475, 2022.
- [20] M. Sharma and M.O. Badawy, "Application of model predictive control in modular multilevel converters for MTPA operation and reduced switching losses," in 2018 7th International Conference on Renewable Energy Research and Applications (ICRERA), IEEE, pp. 1233-1239, October 2018.
- [21] M. Allouche, S. Abderrahim, H.B. Zina, and M. Chaabane, "A novel fuzzy control strategy for maximum power point tracking of wind energy conversion system," *International Journal of Smart Grid-ijSmartGrid*, vol. 3, no. 3, pp. 120-127, 2019.
- [22] R. Tiwari, P. Pandiyan, S. Saravanan, T. Chinnadurai, N. Prabakaran, and K. Kumar, "Quadratic boost converter for wind energy conversion system using back propagation neural network maximum power point tracking," *International Journal of Energy Technology and Policy*, vol. 18, no. 1, pp. 71-89, 2022.
- [23] T. Dinku, T.M. Dinku, and M.S. Manshahia, "Artificial intelligence techniques for modeling of wind energy harvesting systems: a comparative analysis," in *Advances of Artificial Intelligence in a Green Energy Environment*, Academic Press, pp. 173-192, 2022.
- [24] M. Mansoor, Q. Ling, and M.H. Zafar, "Short Term Wind Power Prediction using Feedforward Neural Network (FNN) trained by a Novel Sine-Cosine fused Chimp Optimization Algorithm (SChoA)," in 2022 5th International Conference on Energy Conservation and Efficiency (ICECE), IEEE, 2022.
- [25] M. Alzayed, H. Chaoui, and Y. Farajpour, "Maximum power tracking for a wind energy conversion system using cascade-forward neural networks," *IEEE Transactions on Sustainable Energy*, vol. 12, no. 4, pp. 2367-2377, 2021.
- [26] Y.A. Ali and M. Ouassaid, "Sensorless MPPT Controller using Particle Swarm and Grey Wolf Optimization for Wind Turbines," in 2019 7th International Renewable and Sustainable Energy Conference (IRSEC), IEEE, 2019.
- [27] B.S. Goud, R. Reddy, R.R. Udumula, M. Bajaj, B. Abdul Samad, M. Shouran, and S. Kamel, "PV/WT integrated system using the Gray Wolf Optimization Technique for power quality improvement," *Frontiers in Energy Research*, vol. 10, 2022.
- [28] V. Karthikeyan, "MPPT with Single DC-DC Converter and Inverter for Grid Connected Hybrid Wind-Driven PMSG-PV System Using GA Algorithm," *Renewable Energy with IoT and Biomedical Applications*, vol. 1, 2021, pp. 41.